The Astrophysical Journal, 603:82–86, 2004 March 1

GLOBULAR CLUSTER FORMATION IN M82

S. J. Lipscy and P. Plavchan
Department of Physics and Astronomy, University of California, Box 951547, Knudsen Hall, Los Angeles, CA 90095-1562;
lipscy@astro.ucla.edu, plavchan@astro.ucla.edu
Received 2003 September 25; accepted 2003 November 13

ABSTRACT

We present high-resolution mid-infrared (mid-IR; 11.7 and 17.65 μm) maps of the central 400 pc region of the starburst galaxy M82. Seven star-forming clusters are identified, which together provide ~15% of the total mid-IR luminosity of the galaxy. We find that these young stellar clusters have inferred masses and sizes comparable to globular clusters. At least 20% of the star formation in M82 is found to occur in super star clusters.

Subject headings: galaxies: individual (M82) — galaxies: starburst — galaxies: star clusters — infrared: galaxies

1. INTRODUCTION

M82 (NGC 3034) is often considered the archetypical starburst galaxy, since it has a derived star formation rate (~10 $M_\odot$ yr^{-1}; O'Connell & Mangano 1978) that would deplete the observed molecular gas in $<10^8$ yr (i.e., short on a Hubble timescale; Lord et al. 1996). The starburst phenomenon traces recent star formation, since it is the massive stars (>8 $M_\odot$), which have short lives, that dominate the energetic output of the host galaxy. The nuclear starburst of M82 dominates the infrared (IR) luminosity of the galaxy: essentially all of the galaxy's $L_{\rm IR} \sim 3.6 \times 10^{10}\, L_\odot$[1] comes from the central kiloparsec (Telesco & Harper 1980).

Optical and near-IR imaging of M82 has revealed numerous super star clusters in its active star-forming nucleus. Ground-based optical imaging of the central region detected eight young knots distributed throughout the region (O'Connell & Mangano 1978). Further study of these knots broke them into smaller star clusters (half-light diameters ~3–4 pc) and suggested cluster-dynamical masses of 10^4–$10^6\, M_\odot$ (Smith & Gallagher 2001; de Grijs, O'Connell, & Gallagher 2001; McCrady, Gilbert, & Graham 2003).

M82's current starburst is thought to have been triggered by its interaction with M81 ~10^8 yr ago (Cottrell 1977; Achtermann & Lacy 1995). It has been argued that the conditions resulting from interactions and mergers of galaxies are favorable for globular cluster formation (e.g., Taniguchi, Trentham, & Ikeuchi 1999 and references therein). UV studies of global properties of starbursting galaxies have shown that as much as 20% of the light is produced in the luminous knots (Meurer et al. 1995; Zepf et al. 1999), suggesting a high efficiency of cluster formation in starbursts. Understanding the star formation occurring in M82's nuclear region can provide insight into both the general process of star formation in starburst environments and also the process and efficiency of forming super star clusters.

The nearly edge-on geometry of M82 combined with heavy optical extinction ($A_V \sim 5$–25 mag; Lester et al. 1990; Telesco et al. 1991; Larkin et al. 1994; Satyapal et al. 1995) has made the galaxy's central 400 pc difficult to study. Even in the near-IR where $A_{2.2\,\mu{\rm m}} \sim 1/10 A_V$ (Rieke & Lebofsky 1985), it is difficult to directly measure the deepest star-forming regions. The mid-IR region of the spectrum is essential for probing deep into the central regions of M82 and revealing the details of the intense star formation occurring in the central regions. Previously, the highest resolution mid-IR map of the central region of M82 was a 12.4 μm map by Telesco & Gezari (1992), which had a resolution ~1.″1. Mid-IR maps of M82 with lower resolution have also been published by Rieke et al. (1980), Telesco, Decher, & Joy (1989), Dietz et al. (1989), Telesco et al. (1991) and Förster-Schreiber et al. (2003). In this paper, we present higher resolution 11.7 and 17.65 μm maps of M82. We discuss evidence suggesting the sources in the maps are young counterparts to globular clusters and estimate the efficiency of super star cluster formation in M82.

2. OBSERVATIONS

On 2003 April 23, we imaged M82 at 3.5 (L band), 11.7, and 17.65 μm with the Long Wavelength Spectrograph (LWS; Jones & Puetter 1993), a facility instrument at the W. M. Keck Observatory. LWS uses a 128 × 128 pixel Boeing Si:As detector and has a plate scale of 0.″08 pixel^{-1}, resulting in a 10.″2 × 10.″2 field of view. We used the "chop-nod" mode of observing, with a chop throw of 15″ north. The bad pixels in the images have been smoothed over, and a mask has been applied to remove the portion of the detector not illuminated by the source. The seeing varied during the course of the observations so the resolution in individual frames ranged from 0.″4 to 1.″0 at 11.7 μm and from 0.″5 to 0.″7 at 17.65 μm. At each of seven pointings across M82's nuclear region, we imaged at all three wavelengths before moving to the next pointing. Images from the seven pointings were mosaicked by centroiding on the bright sources in each frame. Assigning coordinates to the field was accomplished by aligning Two Micron All Sky Survey (2MASS) sources with the centroids of the two bright sources in the L-band frames. We estimate that our positions are accurate to ~0.″5. The star μ UMa was used as the primary standard for flux density and point-spread function (PSF) calibration, and α Her and η Sgr were used to estimate a calibration error of ~20%.

3. CHARACTERIZATION OF MID-IR SOURCES

Our mid-IR maps, presented as Figures 1 and 2, contain several bright, resolved sources as well as diffuse emission

[1] Telesco & Harper (1980) published $L_{\rm IR} = L(1$–$300\ \mu{\rm m}) = 3.0 \times 10^{10}\, L_\odot$ assuming a distance to M82 of 3.3 Mpc. We have updated $L_{\rm IR}$ for the distance of 3.6 Mpc used in this paper; see Freedman et al. (1994) and Sakai & Madore (1999).

connecting the brighter sources. The mid-IR sources, labeled A to G from west to east, are denoted by open black circles (with radii 0.″5, corresponding to the positional error). For reference, the 2 μm peak is marked in the figures as a yellow cross (Dietz et al. 1986) and the dynamical center measured by Weliachew, Fomalont, & Greisen (1984) is marked with a yellow circle. The sharp edges visible in the maps (e.g., southeast of source B in the 11.7 μm map) are artifacts that resulted from the mosaicking of images with differing thermal backgrounds and do not affect the results of this paper.

The earlier, lower resolution 12.4 μm map by Telesco & Gezari (1992) contained two bright regions, one to either side of the galaxy's center. The overall structure in our higher resolution maps is comparable, although we identify individual resolved sources within the Telesco & Gezari sources. To compare their flux densities with those previously published, Telesco & Gezari reported a flux of 6.5 $\pm$ 0.7 Jy at 12.4 μm for the 4″ $\times$ 4″ region containing our sources C and D. We measure a flux for the same region of 5.3 $\pm$ 1.3 Jy at 11.7 μm, in agreement with the previous observation.

The flux densities and half-intensity major and minor axes measured from the maps for the mid-IR sources are listed in Table 1. For sources covered by more than one image, photometry was performed on each image individually, and the average of the measurements is presented here. The standard deviation of the measurements due to background variations was $\lesssim$15% and, combined quadratically with the calibration error, results in an overall flux density error of $\lesssim$25% in our measurements.

Using our 11.7 and 17.65 μm flux densities, we estimate the color temperature of the mid-IR–emitting dust to be in the range 150–270 K, assuming the dust particles radiate as blackbodies. The mid-IR luminosities ($L_{\rm MIR} \equiv L_{12-18\ \mu{\rm m}}$) of the sources, estimated by fitting the measured flux densities to a blackbody with the color temperatures for each source, are all between 0.2×10^8 and 6×10^8 $L_\odot$ and sum to 2.4×10^9 $L_\odot$. Estimating the $L_{\rm MIR}$ for the entire galaxy, using the same procedure with the uncorrected *IRAS* 12 and 25 μm flux densities of 53 and 274 Jy respectively, gives 1.7×10^{10} $L_\odot$; thus, the seven mid-IR sources contribute $\sim$15% of M82's total $L_{\rm MIR}$.

Using radio images at five frequencies, Allen (1999) created spectrally decomposed images of thermal (free-free) and nonthermal (synchrotron) emission. We find that not only do all the centers of the thermal H II regions (marked in Figs. 1 and 2 with red squares) match the centers of the mid-IR sources reasonably well, the diffuse structure in the mid-IR maps closely follows the structure in the thermal free-free map. Golla, Allen, & Kronberg (1996) also noted the correspondence of the diffuse 1.5 and 22 GHz emission with the Telesco & Gezari (1992) 12.4 μm emission. This supports the hypothesis that the mid-IR sources are heavily obscured H II regions.

The [Ne II] (12.8 μm) map published by Achtermann & Lacy (1995), with a resolution of $\sim$1″, also correlates well with our mid-IR maps (see Fig. 3). It should be noted that while the peak of the [Ne II] line lies within our 11.7 μm filter bandpass ($\Delta\lambda$ = 2.4 μm), based on the 5–16.5 μm spectra presented in Förster-Schreiber et al. (2003), the [Ne II] line contributes $\lesssim$15% of the flux in our bandpass. We interpret the correlation between the mid-IR and [Ne II] emission as confirmation that the source of the mid-IR emission is dust heated by UV from young stars that ionize Ne I. Further evidence to support this hypothesis comes from the Brγ map from Larkin et al. (1994). Although not covering the entire mid-IR field, the Brγ emission observed is also well correlated with the mid-IR emission. Both emission line maps agree with the mid-IR map in the apparent lack of emission toward the dynamical center of M82.

Nonthermal radio sources from McDonald et al. (2002) and Allen (1999) are shown in Figures 1 and 2 as magenta crosses; these are assumed to be supernova remnants since they have inverted radio spectra. We find no correlation between the radio supernova remnants and the mid-IR sources, but note that most of the supernova remnants follow the outer edge of the mid-IR emission at a flux levels $\lesssim$0.3 Jy arcsec^{-2} at 11.7 μm and $\lesssim$0.7 Jy arcsec^{-2} at 17.65 μm.

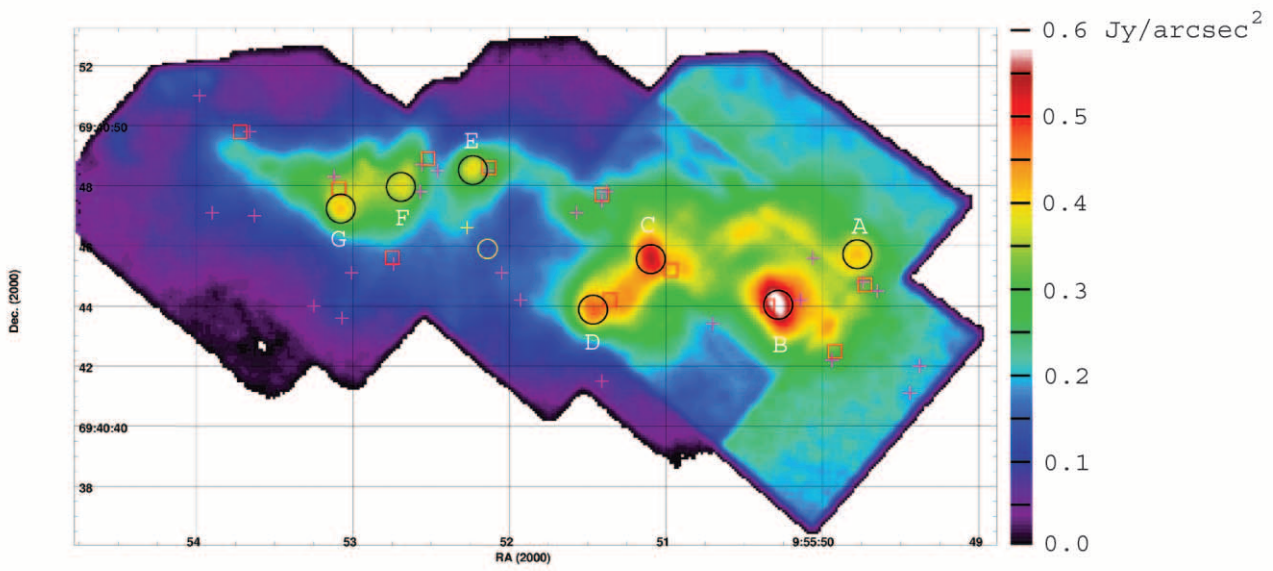

FIG. 1.—Central region of M82 at 11.7 μm smoothed with a 0.″4 boxcar function. The seven mid-IR sources are labeled with white letters and their positional errors are represented by 0.″5 radius open black circles. The 2 μm peak (Dietz et al. 1986) is labeled with a yellow cross, and the dynamical center of M82 as determined by Weliachew et al. (1984) is marked by a yellow circle. Magenta crosses mark positions for nonthermal radio sources (McDonald et al. 2002; Allen 1999), and red squares mark the positions of H II regions (Allen 1999).

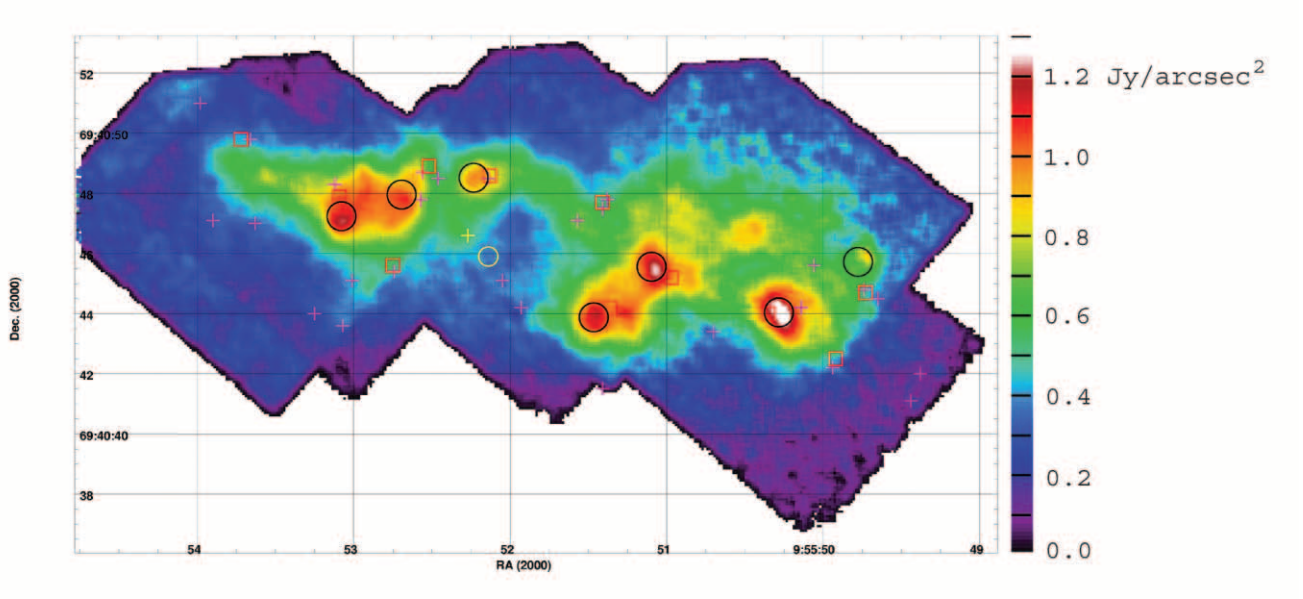

FIG. 2.—Central region of M82 at 17.65 μm smoothed with a 0.″4 boxcar function. Symbols are the same as in Fig. 1.

Following Beck, Turner, & Gorjian (2001), we assume a reference OB star luminosity of $2.5 \times 10^5\ L_\odot$ for an O7 star (Vacca, Garmany, & Shull 1996) to calculate the OB star content of each mid-IR source from its $L_{\rm MIR}$. These values are listed in Table 1. For the brightest regions (B, C, and G) we find that ~2000–2500 O7 stars are required to generate the mid-IR luminosity. Förster-Schreiber et al. (2001) derived comparable numbers of OB stars for regions near sources B and C (3200 and 4400 O7 stars, respectively) using He I : Brγ line ratios to estimate the Lyman continuum flux from their regions.

Since we find that the [Ne II] emission correlates spatially with the mid-IR emission, we use [Ne II] channel maps from Achtermann & Lacy (1995), which have a resolution of 16 km s^{-1}, to estimate velocity dispersions ($\sigma_{\rm vel}$) in the ionized gas of ~15–30 km s^{-1} at the positions of the mid-IR sources. Estimates of the velocity dispersions from the Brγ (Larkin et al. 1994) and ^{13}CO (Neininger et al. 1998) channel maps, each with lower velocity resolution, give similar results. A caveat to using ionized emission to estimate a velocity dispersion is that the ionized gas may well be accelerated by shocks, and therefore its velocity should be considered an upper limit to the stellar velocity.

From the range of estimated velocity dispersions and assuming virialized systems, we use $M = \eta\sigma_{\rm vel}^2 r_h/G$ to calculate a range for the total mass in each these systems. In this formulation, G is the gravitational constant, r_h is the projected half-intensity radius defined to be the geometric mean of the semimajor and semiminor axes, and $\eta = 10$ (Smith & Gallagher 2001). The mass ranges for each mid-IR source are listed in Table 1 and should be considered *upper limits* since H II regions are generally found to be freely expanding systems. For the largest sources, the mass range we find is 6×10^6–$25 \times 10^6\ M_\odot$. In every case, the range contains the system mass found by extrapolating from the number of O7 stars using a Salpeter mass function. Comparing the sizes and masses of the star clusters forming in M82 to three of the

TABLE 1
PROPERTIES OF PROTO–GLOBULAR CLUSTERS IN M82 AND GALACTIC GLOBULAR CLUSTERS

Source	F_ν(11.7 μm) (Jy)	F_ν(17.65 μm) (Jy)	Size[a] (pc)	T_c (K)	$L_{\rm MIR}$ ($10^8\ L_\odot$)	N(O7)	Mass[b]
A	0.16	0.15	10 × 10	270	0.20	80	0.3[c]
B	3.17	5.39	30 × 21	195	5.9	2400	6–25
C	2.38	5.95	26 × 19	165	5.5	2200	6–22
D	1.23	3.31	21 × 12	160	3.3	1300	4–16
E	0.67	1.74	13 × 13	160	1.7	700	3–13
F	0.77	2.24	28 × 8	155	2.3	900	4–15
G	1.56	4.96	25 × 16	150	4.9	2000	5–20
ω Cen	...	...	9[d]	...	...	...	2[e]
NGC 6273	...	...	3[d]	...	...	...	1[e]
NGC 104	...	...	5[d]	...	...	...	1[e]

[a] Sizes are full width at half-intensity major and minor axes of elliptical sources, as observed, and include a ~0.″5 (9 pc) PSF.
[b] Upper limit to mass of systems.
[c] Source A is not identifiable in the [Ne II] channel maps. Stellar mass was extrapolated from the number of O7 stars using a Salpeter initial mass function.
[d] Sizes are averages of values in van den Bergh, Morbey, & Pazder 1991 and Mandushev et al. 1991.
[e] From Mandushev et al. 1991.

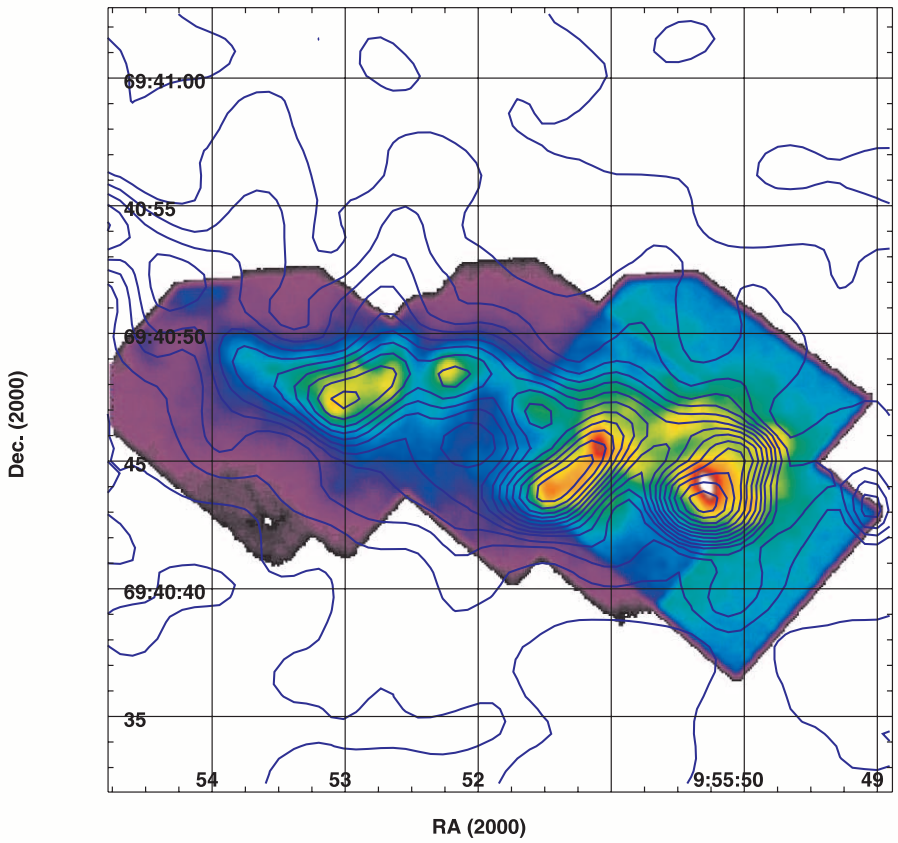

FIG. 3.—Smoothed 11.7 μm data overlaid with contours from the Achtermann & Lacy (1995) [Ne II] line map deconvolved with the maximum entropy method (their Fig. 5).

largest Galactic globular clusters, which have radii of 5–10 pc and masses of 1×10^6–$2 \times 10^6\ M_\odot$ (see Table 1), we conclude that the star clusters forming in the nuclear region of M82 are young analogs to globular clusters.

The existence of present-day globular cluster sized knots of star formation is not unique to M82. Indeed, super star clusters containing quantities of OB stars similar to those we find in M82 have been observed in a number of galaxies (e.g., NCG 5253 in Turner et al. 2003; He 2-10 in Johnson & Kobulnicky 2003; NGC 4038/9 in Mengel et al. 2002). In addition, two star-forming regions in the Milky Way, the Arches cluster near the Galactic center and the Cygnus OB2 association, are estimated to each weigh in at $6 \times 10^4\ M_\odot$ (Serabyn, Shupe, & Figer 1998; Knödlseder 2000), comparable to a small globular cluster (Mandushev, Staneva, & Spasova 1991; Pryor & Meylan 1993). However, the Arches cluster and Cygnus OB2 each contain around 100 O stars, which contribute together only ~3% of the total Galactic O stars (Terzian 1974), and yet far outnumber all other Galactic star-forming regions in their O star content.

In M82, the seven mid-IR sources in the nuclear region together contribute ~15% of the total $L_{\rm MIR}$ of the galaxy. The [Ne II] map suggests that there may be several H II regions outside our mid-IR field that may contribute up to an additional ~5% to the total $L_{\rm IR}$. Assuming all the mid-IR luminosity in M82 comes from star formation (Telesco 1988), it follows that $\gtrsim$20% of M82's star formation is in the form of super star clusters, in contrast to the mere 3% in the Milky Way. This may be an important feature of starbursts in general; not only do they provide an environment suitable for forming globular clusters, but the super star cluster formation efficiency in starbursts is $\gtrsim$20%.

4. CONCLUSIONS

This paper presents mid-IR (11.7 and 17.65 μm) maps with ~0.″5 resolution of the central 400 pc of the starbursting galaxy M82. We find seven resolved sources in this region of M82 with luminosities summing to 15% of the total *IRAS* flux of the entire galaxy. The mid-IR maps exhibit features comparable to those found in maps of [Ne II] emission, Brγ emission, and thermal free-free emission. We present evidence implying that the mid-IR sources are giant H II regions in which globular cluster sized star clusters are forming. Our data imply that $\gtrsim$20% of the star formation in M82 is occurring in super star clusters.

This work has been supported by funding from NASA. The authors wish to thank Mike Jura, Jean Turner, and James Larkin for helpful comments. Data presented here were obtained at the W. M. Keck Observatory, which is operated as a scientific partnership among the California Institute of Technology, the University of California, and NASA. The Observatory was made possible by the generous financial support of the W. M. Keck Foundation. The authors

wish to recognize and acknowledge the very significant cultural role that the summit of Mauna Kea has always had within the indigenous Hawaiian community. We are most fortunate to have the opportunity to conduct observations from this mountain. This publication makes use of data products from the Two Micron All Sky Survey, which is a joint project of the University of Massachusetts and the Infrared Processing and Analysis Center/California Institute of Technology, funded by the NASA and the National Science Foundation.

REFERENCES

Achtermann, J. M., & Lacy, J. H. 1995, ApJ, 439, 163
Allen, M. L. 1999, Ph.D. thesis, Univ. Toronto
Beck, S. C., Turner, J. L., & Gorjian, V. 2001, AJ, 122, 1365
Cottrell, G. A. 1977, MNRAS, 178, 577
de Grijs, R., O'Connell, R. W., & Gallagher, J. S. 2001, AJ, 121, 768
Dietz, R. D., Gehrz, R. D., Jones, T. J., Grasdalen, G. L., Smith, J., Gullixson, C., & Hackwell, J. A. 1989, AJ, 98, 1260
Dietz, R. D., Smith, J., Hackwell, J. A., Gehrz, R. D., & Grasdalen, G. L. 1986, AJ, 91, 758
Förster-Schreiber, N. M., Genzel, R., Lutz, D., Kunze, D., & Sternberg, A. 2001, ApJ, 552, 544
Förster-Schreiber, N. M., Sauvage, M., Charmandaris, V., Laurent, O., Gallais, P., Mirabel, I. F., & Vigroux, L. 2003, A&A, 399, 833
Freedman, W. L. et al. 1994, ApJ, 427, 628
Golla, G., Allen, M. L., & Kronberg, P. P. 1996, ApJ, 473, 244
Johnson, K. E., & Kobulnicky, H. A. 2003, ApJ, 597, 923
Jones, B., & Puetter, R. C. 1993, Proc. SPIE, 1946, 610
Knödlseder, J. 2000, A&A, 360, 539
Larkin, J. E., Graham, J. R., Matthews, K., Soifer, B. T., Beckwith, S., Herbst, T. M., & Quillen, A. C. 1994, ApJ, 420, 159
Lester, D. F., Carr, J. S., Joy, M., & Gaffney, N. 1990, ApJ, 352, 544
Lord, S. D., Hollenbach, D. J., Haas, M. R., Rubin, R. H., Colgan, S. W. J., & Erickson, E. F. 1996, ApJ, 465, 703
Mandushev, G., Staneva, A., & Spasova, N. 1991, A&A, 252, 94
McCrady, N., Gilbert, A. M., & Graham, J. R. 2003, ApJ, 596, 240
McDonald, A. R., Muxlow, T. W. B., Wills, K. A., Pedlar, A., & Beswick, R. J. 2002, MNRAS, 334, 912
Mengel, S., Lehnert, M. D., Thatte, N., & Genzel, R. 2002, A&A, 383, 137
Meurer, G. R., Heckman, T. M., Leitherer, C., Kinney, A., Robert, C., & Garnett, D. R. 1995, AJ, 110, 2665
Neininger, N., Guelin, M., Klein, U., Garcia-Burillo, S., & Wielebinski, R. 1998, A&A, 339, 737
O'Connell, R. W., & Mangano, J. J. 1978, ApJ, 221, 62
Pryor, C., & Meylan, G. 1993, in ASP Conf. Ser. 50, Structure and Dynamics of Globular Clusters, ed. S.G. Djorgovski, & G. Meylan (San Francisco: ASP), 357
Rieke, G. H., & Lebofsky, M. J. 1985, ApJ, 288, 618
Rieke, G. H., Lebofsky, M. J., Thompson, R. I., Low, F. J., & Tokunaga, A. T. 1980, ApJ, 238, 24
Sakai, S., & Madore, B. F. 1999, ApJ, 526, 599
Satyapal, S., et al. 1995, ApJ, 448, 611
Serabyn, E., Shupe, D., & Figer, D. F. 1998, Nature, 394, 448
Smith, L. J., & Gallagher, J. S. 2001, MNRAS, 326, 1027
Taniguchi, Y., Trentham, N., & Ikeuchi, S. 1999, ApJ, 526, L13
Telesco, C. M. 1988, ARA&A, 26, 343
Telesco, C. M., Campins, H., Joy, M., Dietz, K., & Decher, R. 1991, ApJ, 369, 135
Telesco, C. M., Decher, R., & Joy, M. 1989, ApJ, 343, L13
Telesco, C. M., & Gezari, D. Y. 1992, ApJ, 395, 461
Telesco, C. M., & Harper, D. A. 1980, ApJ, 235, 392
Terzian, Y. 1974, ApJ, 193, 93
Turner, J. L., Beck, S. C., Crosthwaite, L. P., Larkin, J. E., McLean, I. S., & Meier, D. S. 2003, Nature, 423, 621
Vacca, W. D., Garmany, C. D., & Shull, J. M. 1996, ApJ, 460, 914
van den Bergh, S., Morbey, C., & Pazder, J. 1991, ApJ, 375, 594
Weliachew, L., Fomalont, E. B., & Greisen, E. W. 1984, A&A, 137, 335
Zepf, S. E., Ashman, K. M., English, J., Freeman, K. C., & Sharples, R. M. 1999, AJ, 118, 752